Experimental Control of Cardiac Muscle Alternans

G. Martin Hall* and Daniel J. Gauthier†

Department of Physics, Department of Biomedical Engineering and Center for Nonlinear and Complex Systems, Duke University, Box 90305, Durham, North Carolina 27708

(Received 26 July 2001; published 30 April 2002)

We demonstrate that alternans in small pieces of *in vitro* paced bullfrog *(Rana Catesbeiana)* myocardium can be suppressed by making minute adjustments to the pacing period in response to real time measurements of the action potential duration. Control is possible over a large range of physiological conditions over many animals and the self-referencing control protocol can automatically adjust to changes in the pacing interval. Our results suggest the feasibility of developing low-energy methods for maintaining normal cardiac function.

DOI: 10.1103/PhysRevLett.88.198102 PACS numbers: 87.15.Aa, 05.45.–a, 87.10.+e

Alternans is a periodic cardiac rhythm in which the duration of the muscle contractions alternate in a pattern $ABAB\ldots$ [1]. This rhythm can trigger the onset of fibrillation [2], a state where the average heart rate is elevated and muscle contractions at one point of the heart are uncoordinated with other points. Fibrillation is believed to be a manifestation of the deterministic behavior known as spatiotemporal chaos [3], and it may be possible to prevent its occurrence by placing controllers [4] in direct contact with the cardiac muscle at a few or many spatial locations [5]. One promising study suggests that *in vivo* human atrial fibrillation can be stabilized by applying control at only a single spatial location [6].

Alternans is also known to occur in re-entrant atrioventricular nodal conduction. This arrhythmia occurs when electrical signals from the atria pass through the atrioventricular node (essentially a one-dimensional conduction pathway) into the ventricles and back to the atria via an abnormal conduction pathway. Atrioventricular nodal dynamics are known to be well described by a one-dimensional map-based mathematical model [7] and hence are expected to be amenable to control. Indeed, feedback control methods have been used recently to suppress atrioventricular nodal conduction alternans in an *in vitro* rabbit heart model [8] and in an *in vivo* human heart model [7].

On the other hand, controlling cardiac muscle dynamics is expected to be more difficult because previous research [9] suggests that the dynamics are more complicated (higher dimensional) than atrioventricular nodal dynamics. In fact, the first pioneering experiments that used closed-loop feedback to control *in vitro* the dynamics of irregular cardiac rhythms in a piece of the interventricular septum of a rabbit heart [10] could not successfully stabilize the desired rhythm.

The primary purpose of this Letter is to present experimental results demonstrating that cardiac muscle alternans can be suppressed in small pieces of *in vitro* paced bullfrog cardiac muscle using a simple self-referencing scheme. Once alternans is suppressed, the size of the control perturbations are very small, limited by noise and slight imperfections in the controller. Control is possible over the entire range of observed alternans and for a wide range of control parameters, and we demonstrate that the controller can automatically track changes in the pacing interval. In addition, we repeat the experiment using several animals, demonstrating that the control protocol can handle significant animal-to-animal variation [9]. We also point out that such control experiments provide a new tool for cardiac-model verification.

The key idea underlying the control of alternans is to design perturbations that stabilize the system about one of the unstable equilibrium states embedded in the system [4]. The corresponding unstable equilibrium state in our experiments is a 1:1 (or period-1) pattern [11,12] for which the action potential duration (APD) is the same for each stimulus, denoted by APD^*. The APD is the time for cells to repolarize after depolarization by a pacing stimulus. This state can be stabilized by making small real-time adjustments to the pacing interval PI based on measurements of the APD using the setup shown in Fig. 1a. Stabilizing any other dynamical state requires large repeated adjustments to PI. An example of a 1:1 response pattern for long PI

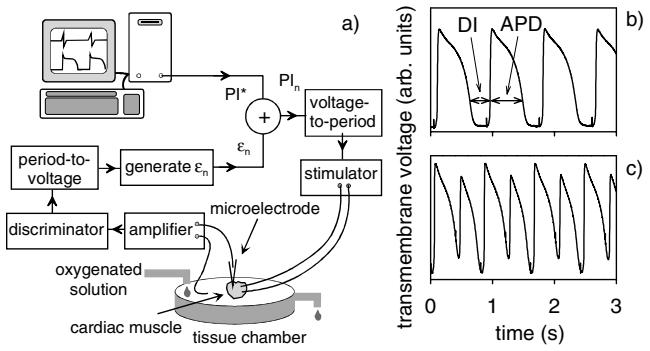

FIG. 1. (a) Experimental setup for controlling alternans in small pieces of paced cardiac muscle. Temporal evolution of the transmembrane voltage displaying (b) a 1:1 response pattern for a slow pacing interval with $PI^* = 850$ ms and (c) an alternans response pattern for rapid pacing with $PI^* = 400$ ms. The arrows in (b) indicate the action potential duration APD and the diastolic interval DI.

for which this pattern is stable is shown in Fig. 1b, and an example of alternans under conditions of rapid pacing is shown in Fig. 1c. Note that APD* is in between the two values of APD shown in this figure.

To suppress alternans and produce a stable 1:1 pattern, we adjust the pacing period by an amount given by [8,13,14]

$$\varepsilon_n = -\gamma(\mathrm{APD}_{n-1} - \mathrm{APD}_{n-2}), \quad (1)$$

where APD_m is the APD at the mth observation and γ is the feedback gain. The controller requires no mathematical model, and it is self-referencing in that it uses the past behavior of the system as an approximation APD*. Control is initiated by adjusting $\mathrm{PI}_n = \mathrm{PI}^* + \varepsilon_n$, where PI* is the nominal pacing period. When control is successful, $\varepsilon_n \simeq 0$, and $\mathrm{PI}_n \simeq \mathrm{PI}^*$.

The time sequence of one of our typical control experiments [15] is shown in Fig. 2a where we plot APD_n and $\varepsilon_n/\mathrm{PI}^*$ as a function of the pace index n. Before control is initiated, the APD's alternate between approximately 100 and 220 ms. After control is turned on, APD_n undergoes a complex transient *en route* to the desired 1:1 state. Initially, the control perturbations are large but diminish rapidly, as seen in Fig. 2b. Once the state is stabilized, $\mathrm{PI}_n \simeq \mathrm{PI}^*$, $\mathrm{APD}_n \simeq \mathrm{APD}^* \simeq 159$ ms, and $\varepsilon_n/\mathrm{PI}^* \lesssim 10^{-3}$, indicating that we have stabilized a true underlying unstable state of the system via the minute control perturbations. After control is turned off, the dynamics slowly leaves the neighborhood of the 1:1 state as the tissue returns to alternans. Observing this return to alternans gives valuable information concerning the stability of the 1:1 state that cannot be obtained using typical pacing protocols. For example, we find that the Floquet multiplier characterizing the growth of deviations of APD^n about APD* is approximately equal to 1.38 for this data set.

We have obtained similar results over many trials. Out of 40 animals studied, 18 displayed alternans [9]. In 2 out of these 18 animals, technical difficulties in the experiment prevented application of control. In 14 out of the remaining 16 animals, it was possible to suppress alternans and produce the desired 1:1 state using the feedback algorithm over essentially the entire range of PI*'s displaying alternans in the absence of control. During successful control, the typical variation of APD_n was reduced to less than 2% of APD* from an alternation of as much as 60% of APD* in the absence of control.

To demonstrate the control efficacy, we measure the tissue response as PI* is varied. The bifurcation diagram shown in Fig. 3a illustrates the baseline response in the absence of feedback perturbations ($\gamma = 0$). It is generated by recording APD_n while adjusting PI* from 1200 to 300 ms in 50 ms intervals. For each PI*, the response of the tissue to the first 5–10 stimuli is discarded in order to eliminate transients and the subsequent behavior is recorded for up to 10 s. The width of each action potential is determined at 70% of full repolarization and plotted at

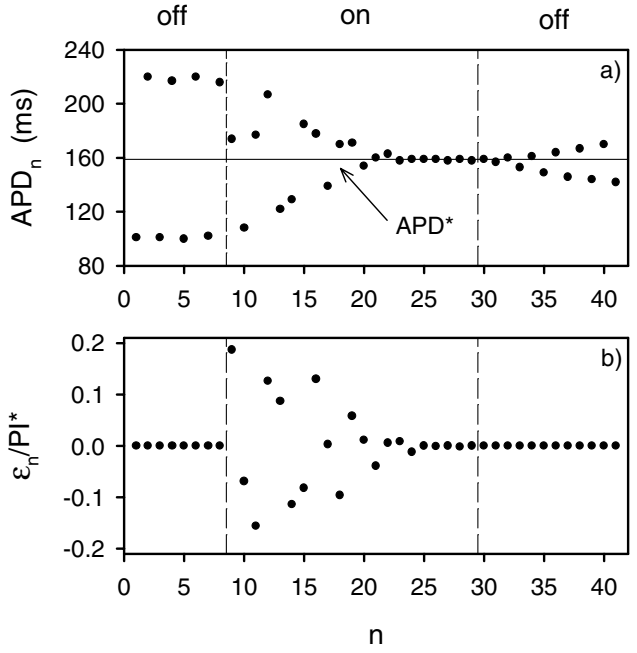

FIG. 2. Typical control sequence in which the feedback adjustments to the pacing period are applied for approximately 10 s with $\gamma = 1.52$. Action potential duration (a) and feedback error signal (b) as a function of the beat number for $\mathrm{PI}^* = 500$ ms. The dashed vertical lines indicate the moment when control is turned on or off.

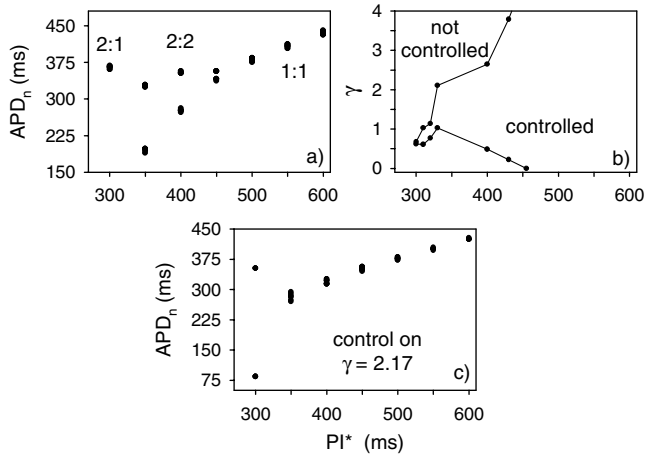

FIG. 3. The range of control of alternans (for a different animal than the one used to collect the data in Fig. 2 but the same for the one in Fig. 1). (a) Bifurcation diagram in the absence of control illustrating the transition from the period-1 (or 1:1) response pattern, to alternans (2:2), and eventually to a 2:1 pattern as the pacing interval is decreased. (b) The domain of control (to the right of the line) is determined by setting PI* and adjusting γ while monitoring ε_n. The cutoff to determine successful control is set at $\varepsilon_n/\mathrm{PI}^* = 2\%$. (c) Observed bifurcation diagram when control is turned on initially at long PI* with $\gamma = 2.17$ in the presence of closed-loop feedback control with no adjustments made to the controller during the entire experiment.

each PI*. From the diagram, it is seen that only one value of APD appears for long PI*, indicating a stable 1:1 pattern. For decreasing PI*, the APD shortens consistent with the restitution properties of cardiac muscle. At PI* $\approx$ 455 ms, a transition from a 1:1 to a 2:2 pattern occurs, known as a bifurcation. For shorter PI* the APD's alternate between short and long values. At PI* $\approx$ 310 ms, a transition to a 2:1 behavior occurs, where one action potential is elicited for every two stimuli [9].

We find that the desired 1:1 pattern can be produced for a range of feedback gains, as summarized by the "domain of control" shown in Fig. 3b. In this plot, control is achieved for all values of γ to the high-PI side of the line. It is seen that control is possible over a wide range of γ's until the domain pinches down near the transition to the 2:1 behavior. Because of this wide range of γ's, control can be initiated without precise *a priori* knowledge of the optimal γ for the system, and the controller can automatically track changes in APD* as the tissue properties change. This tracking ability is shown in Fig. 3c where we generate a bifurcation diagram with the controller turned on. It is seen that the 1:1 behavior is produced over essentially the entire observed range of alternans in the absence of control.

Besides the potential clinical implications of our experiments [7], we find that controlling alternans provides a new experimental tool for assessing the veracity of mathematical models of cardiac dynamics. As an example, we consider a one-dimensional map-based model of cardiac dynamics that is often used to treat the bifurcation from 1:1 to 2:2 response patterns [11,12]. The model can be expressed as $\mathrm{APD}_{n+1} = f(\mathrm{DI}_n)$, where f is known as the restitution function, the nth diastolic interval is given by $\mathrm{DI}_n = N \times \mathrm{PP}_n - \mathrm{APD}_n$, PP_n is the period of the applied (nominally periodic) stimulus, N is the smallest integer satisfying $\mathrm{DI}_n > \mathrm{DI}_{\mathrm{min}}$, and $\mathrm{DI}_{\mathrm{min}}$ is the minimum diastolic interval the tissue can sustain. For some tissue preparations, including bullfrog myocardium [9,11], a function of the form $f(\mathrm{DI}_n) = A_1 - A_2 \exp(-DI_n/\tau_1)$ gives reasonable agreement with experimental observations and displays alternans under appropriate conditions, where A_1, A_2, and τ_1 are tissue-dependent constants. While this simple model is known to have limitations, it is appealing because it captures many essential features of myocardium response without great mathematical complexity, and hence it often forms the basis of our intuitive understanding of cardiac dynamics.

We compare the observed and predicted bifurcation diagrams by adjusting the model parameters to obtain the best fit between the observed and predicted bifurcation diagrams using the following procedure. We determine two of the model parameters by forcing the predicted value of the bifurcation from 1:1 to 2:2 response patterns to occur at the same pacing interval and action potential duration as observed in the experiment. The remaining parameter governs the range of PI's over which alternans occurs. We chose the parameter value that maximizes this range. This

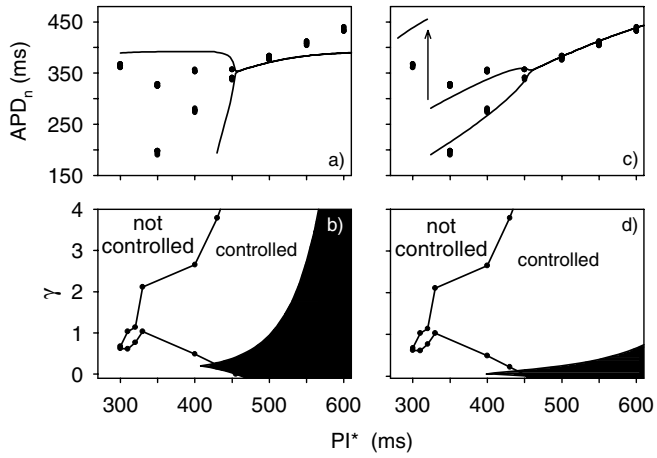

FIG. 4. Comparison between the experimental observations and the predictions of two map-based models of cardiac dynamics. Comparison of the (a) bifurcation diagram and (b) domain of control to the one-dimensional model with parameters $A_1 = 392.0$ ms, $A_2 = 525.3$ ms, $\tau_1 = 40.0$ ms, and $\mathrm{DI}_{\mathrm{min}} = 35.0$ ms. The predictions of the model are shown as a solid line in (a) and the black shaded region in (b). Comparison of the (c) bifurcation diagram and (d) domain of control to the two-dimensional model with parameters $A_1 = 490.9$ ms, $A_2 = 569.0$ ms, $\tau_1 = 64.0$ ms, $\tau_2 = 38.0$ ms, and $\mathrm{DI}_{\mathrm{min}} = 38.0$ ms.

fitting procedure converges rapidly, and there does not exist another set of distinct parameters that fit equally well. It is seen in Fig. 4a that the model accurately captures the bifurcation point but little else. The model fails because it predicts that the 1:1 response pattern should be unstable when $df/d\mathrm{DI} > 1$, whereas the 1:1 pattern observed in our experiment remains stable even when the dynamic restitution curve has a slope greater than one. This observation demonstrates that the cardiac muscle dynamics (i.e., APD_{n+1}) cannot be described by a function that is an explicit function of only DI_n. It is also seen in Fig. 4b that the predicted domain of control (shown as the black shaded region) is limited to PI* near the bifurcation point or to longer values, in disagreement with the experimental observations.

Taking our example one step further, we consider a two-dimensional map of cardiac dynamics [16] that generalizes the one-dimensional model [11,12] by explicitly accounting for rate-dependent changes in the tissue restitution properties [17]. The mapping is given by

$$\mathrm{APD}_{n+1} = (1 - M_n) f(\mathrm{DI}_n), \tag{2}$$

$$M_{n+1} = [1 - (1 - M_n)\exp(\mathrm{APD}_n/\tau_2)]\exp(-\mathrm{DI}_n/\tau_2), \tag{3}$$

where τ_2 is an additional tissue-dependent parameter, and M_n is a "memory" variable.

We compare our observations to this model by adjusting the parameters to force the map to undergo the transition to alternans at the same PI* and for the same value of APD* observed in the experiment and by a nonlinear least squares minimization for the remaining parameters. As seen in

Fig. 4c, the mapping adequately predicts the observed dynamics ($\chi^2_\nu = 3.3, \nu = 74$). Based on this observation, one might be tempted to conclude that the model properly accounts for the observed dynamics and hence should also reasonably predict the observed domain of control. As with the one-dimensional model, this fitting procedure converges rapidly to a distinct set of parameters, and there does not exist another set that fits equally well. Surprisingly, the predicted and observed domain of control are in poor agreement, as seen in Fig. 4d. The predicted domain (black shaded region) is limited to PI* near the bifurcation point and encompasses only a small range of γ's. Hence, fitting the predictions of a model to both the observed bifurcation diagram and domain of control gives additional constraints when undertaking model development. While we have compared our experiments only to highly simplified mathematical models, we suggest that this general procedure will be useful for adjusting the parameters of more realistic, but highly complex, ionic-based models of cardiac dynamics.

In conclusion, we have demonstrated that alternans can be suppressed in small pieces of cardiac muscle using a nonlinear-dynamics-based feedback pacing protocol. Controlling heart dynamics driven by internal pacemaker cells may be possible with modifications to the protocol [6], opening up the possibility of using it to maintain normal heart function in humans via implantable devices [7].

We gratefully acknowledge financial support of the National Science Foundation (PHY-9982860) and the Whitaker Foundation, as well as discussions with Sonya Bahar, Wanda Krassowska, Soma Sau, David Schaeffer, and Joshua Socolar.

*Present address: Corvis Corp., 7015 Albert Einstein Drive, Columbia, MD 21046-9400.
†Corresponding author.
Email address: gauthier@phy.duke.edu.

[1] G. R. Mines, J. Physiol. (London) **46**, 349 (1913).
[2] A. Karma, Chaos **4**, 461 (1994); N. A. M. Estes *et al.,* Am. J. Cardiol. **80**, 1314 (1997).
[3] L. Glass, Phys. Today **49**, No. 8, 40 (1996); A. T. Winfree, Chaos **8**, 1 (1998); F. X. Witkowski *et al.,* Nature (London) **392**, 78 (1998); R. A. Gray, A. M. Pertsov, and J. Jalife, Nature (London) **392**, 75 (1998).
[4] T. Shinbrot, C. Grebogi, E. Ott, and J. A. Yorke, Nature (London) **363**, 411 (1993).
[5] V. N. Biktashev and A. V. Holden, Proc. R. Soc. London B **261**, 211 (1995); L. Glass and M. E. Josephson, Phys. Rev. Lett. **75**, 2059 (1995); M. Watanabe and R. F. Gilmour, Jr., J. Math. Biol. **35**, 73 (1996); D. J. Christini and J. J. Collins, Phys. Rev. E **53**, R49 (1996); W. J. Rappel, F. Fenton, and A. Karma, Phys. Rev. Lett. **83**, 456 (1999); S. Sinha, A. Pande, and R. Pandit, Phys. Rev. Lett. **86**, 3678 (2001).
[6] W. L. Ditto *et al.,* Int. J. Bifurcation Chaos Appl. Sci. Eng. **10**, 593 (2000).
[7] D. J. Christini *et al.,* Proc. Natl. Acad. Sci. U.S.A. **98**, 5827 (2001).
[8] K. Hall *et al.,* Phys. Rev. Lett. **78**, 4518 (1997).
[9] G. M. Hall, S. Bahar, and D. J. Gauthier, Phys. Rev. Lett. **82**, 2995 (1999).
[10] A. Garfinkel, M. L. Spano, W. L. Ditto, and J. L. Weiss, Science **257**, 1230 (1992).
[11] J. B. Nolasco and R. W. Dahlen, J. Appl. Physiol. **25**, 191 (1968).
[12] M. Guevara, G. Ward, A. Shrier, and L. Glass, in *Computers in Cardiology* (IEEE Computer Society, Los Angeles, CA, 1984), p. 167.
[13] D. J. Gauthier and J. E. S. Socolar, Phys. Rev. Lett. **79**, 4938 (1997).
[14] J. E. S. Socolar and D. J. Gauthier, Phys. Rev. E **57**, 6589 (1998).
[15] All procedures are approved by the Duke University Institutional Animal Care and Use Committee (IACUC). The experimental procedure for preparing the tissue is identical to that described in Ref. [9]. We determine the APD by measuring the transmembrane voltage within 1–2 mm of the stimulus electrodes using a glass microelectrode or by measuring a monophasic action potential (MAP) within 2–3 mm of the stimulus electodes using a suction-type electrode. The transmembrane voltage or the MAP signal is amplified, and the APD is determined in real time at 70% of the peak height.
[16] D. R. Chialvo, D. C. Michaels, and J. Jalife, Circ. Res. **66**, 525 (1990).
[17] R. F. Gilmour, Jr., N. F. Otani, and M. A. Watanabe, Am. J. Physiol. **272**, H1826 (1997); F. H. Fenton, S. J. Evans, and H. M. Hastings, Phys. Rev. Lett. **83**, 3964 (1999).